INVESTIGATION OF THE AIRFLOW AROUND AIRCRAFT MODEL AT HIGH AND INTERMEDIATE ANGLE OF ATTACK WITH PRESSURE SENSITIVE PAINT.

A.Bykov, S.Fonov, V. Mosharov, A.Orlov,
V.Pesetsky, V.Radchenko
Central Aero-Hydrodynamics Institute, Zhukovsky, Russia

Abstract.

In recent experiments we demonstrated the feasibility of using the luminescent Pressure Sensitive Paint (PSP) for surface pressure measurements in aerodynamic testing of the models at high and intermediate angle of attack. In practice the airflow at high angle of attack is accompanied by unsteady phenomena- local pressure field oscillations and flow structure reconstruction. PSP gives unique possibility to obtain quantitative results about total pressure field in time and extract information about steady and unsteady input in the resulting aerodynamic loads.

Tests were performed in TsAGI's T104, T106 and T112 wind tunnels using paint formulations, data acquisition and processing systems developed in TsAGI. Pressure measurements were acquired for model of the wing with winglet, for model of maneuverable aircraft at Mach number range 0.6-0.9 and profan blades at velocities up to 6000 revolution per minute. Angles of attack were in the range -4° to 20°. Image acquisition rate was up to 25 frames per second and PSP response time at 99% level was about 0.1-0.3 second, depending on local thickness of the luminescent active layer. The experimental methodology, including data acquisition and processing algorithms, along with the results were described and analyzed.

Introduction

Pressure Sensitive Paint technology recently developed in throughout the world of aerodynamic research centers gives very versatile tool for extensive investigation of flow phenomena around wing at high and intermediate angle of attack.[9,11,14,15,17-21] These flow regimes are accompanied by pike decompression zone near leading edge with complex shock wave structure at subsonic velocities, flow separation from the leading edge or as a result of shock interaction with boundary layer, etc. Usually this three dimensional flow field structure is overcomplicated in third - time dimension, by some non stationary effects. PSP provides possibility of quantitative visualization not only the panoramic pressure field on the total model but its time evolution.

Time domain measurements of two dimensional fields sharply increases requirements to the components of an acquisition system and pressure sensitive paint to be used. Recent achievements in the high speed digital CCD cameras coupled with powerful image processing system, PSP formulations with short response time and experimental experience proves this capability.

In this report we summarized some results of PSP application for non stationary pressure field investigations. These experiments were conducted in TsAGI's wind tunnels, listed here in chronological order: T112 - testing of the model of wing with winglet, T106 - the upper wing surface of training aircraft model, T104 - propeller blade testing.

The concept of using wing-tip plates or winglets to reduce the induced drag of an airplane has been known for many years ago. Interest in study and aerodynamic design of these devices was renewed by Whitcomb's wind tunnel data in 1976, which demonstrated winglets produced a significant gain in the lift-to-drag ratio of a current jet transport.[1] The extensive investigations was performed in the followed time to find out the effect of winglets on jet airplanes over the complete range of flight conditions. Mainly they were the wind tunnel tests which showed not only how the aerodynamics characteristics as induced drag, load distribution and wing root bending moment have been shifted, but pressure distribution on the wing tip and on the winglet also.[2,3]

The detailed test data were followed by numerical calculations performed by vortex lattice method or other panel type methods that allow to study a dependence of the aerodynamics characteristics from such wing and winglet parameters as planform, relative position, airfoil section and twist distribution.[4] A lot of results of this type can be found in paper.[5] All of these methods describe the flow well enough on the whole but details of the pressure distribution near the wing-winglet juncture and a local flow separation can not be caught. The situation is aggravated when shock waves arise in supersonic region or a moderate separation occurs at off-design conditions. Therefore the wind tunnel test to obtain the real pressure distribution in the wing-winglet juncture region must be a part of a winglet aerodynamic design procedure. The PSP method is suitable and informative enough for these purposes. In this report we presents only some results of carefully studying of flows over the wing with winglet from in transonic wind tunnel T-112.[5]

One of the attractive feature of PSP technology is possibility to investigate pressure field on the first stage of the aircraft design using simple aircraft model. New concept of jet training aircraft was investigated in TsAGI's T-106 wind tunnel in very wide range of angle of attack. Pressure field measurements were provided by PSP.

Test section of T106 wind tunnel is instrumented with Optical Pressure Measurement System (OPMS). We can say that T106 wind tunnel is the test bed for PSP technology and OPMS in TsAGI.

The third part of this report presents the using of PSP technology on rotating propellers. Investigation of pressure distribution on propeller blade is necessary for the analysis of the flow about blade and for the testing of calculation methods, used for determination of aerodynamic, acoustic and strength characteristics of propellers. Specific feature of the flow about blade is the presence of radial flow in the boundary layer and in the stall zone. Action of centrifugal and Coriolis forces on this radial flow affects on initialization and evolution of stall zones, and thus on the characteristics of propeller. Also positions and parameters of shock waves on the blade of propeller at transonic velocities depend on radial non uniformity of local flow speed, and thus is the matter of interest.

Pressure field measurement on the blade surface is extremely complicated problem of experimental aerodynamics. Classical technique, i.e., construction of propeller model with a vast amount of pressure taps for surface pressure distribution measurements and solution of data acquisition problem, is quite time-consuming, complex and expensive.[8] PSP-technology provide alternative, quite rapid and economical method to obtain pressure distribution on the rotating propellers.

Measurement Concept.

Luminescence intensity I of PSP-coating is inversely proportional to the pressure p and is directly proportional to excitation light intensity and to the coating thickness. To exclude the influence of excitation light intensity and coating thickness to the measurement result, the ratio of reference image at known (wind-off) condition to operating image at unknown (wind-on) condition must be taken.[9] The surface pressure in the point i can be determined from PSP calibration characteristic:

$$p(i) = A + B\, I_{ref}(i) / I(i) + C(I_{ref}(i) / I(i))^2.$$

Coefficients A, B and C are determined from PSP calibration in laboratory and are assumed to be the same for all points of PSP-coating. Above expression also assumes that: a) model position and shape at wind-on condition is the same as at wind-off condition; b) excitation light distribution remains the same during the test; c) excitation light energy at wind-on exposition is equal to the energy at wind-off exposition; d) there are not any scattering particles in the airflow and on the model surface (dust, fog, smoke etc.) .[9]

Application of PSP-technology for moving objects as the propellers has some specific features.[24] The main problem is image acquisition of moving blade. Linear speed of the blade tip can reach up to 200÷300 m/sec. To eliminate the blade displacement during image acquisition the measurement time must not exceed 1÷2μ sec, that corresponds to the blade tip displacement 0.2÷ 0.5 mm. Longer measurement time causes the loss of spatial resolution. It is problematic to provide so fast image acquisition with continuous excitation light source. More attractive is to use pulsed light source while image detector operates in integration mode. Light sources of two kinds may be used for such measurements: short duration flash lamp and pulsed laser. Depending on light pulse energy, lamp or laser can be used in single pulse mode or in stroboscopic one. Light pulse must be initialized at certain propeller position, so some synchronization system, triggering light source at certain propeller position, is needed. An error of light pulse initialization must not exceed 1÷2μsec to avoid the change in excitation light intensity distribution at wind-on and wind-off conditions and, in case of stroboscopic mode, to avoid the loss of spatial resolution.

The other parameter affecting the image acquisition time is luminescence decay time of PSP after excitation light pulse. This parameter determines spatial resolution of pressure measurement in the same manner as excitation light pulse duration. To provide suitable spatial resolution, luminescence decay time of PSP must not exceed 1 msec (e-time luminescence intensity decay). For example, pressure sensitive paints based on the platinum octaethylporphyrine (PtOEP) are unsuitable for pressure measurement on rotating propellers, as PtOEP has decay time at the zero pressure about 100μsec, i.e. at the test conditions in the range of 20÷50μsec.[15-17,22] So large decay time would cause displacement of the blade tip on the image of 10÷30 mm, that is unsuitable for the pressure measurement on rotating propeller.

The second specific feature is that the propeller rotation is a periodic process of sufficiently high frequency, up to 100÷150 Hz. Airflow directed at some angle of attack to propeller causes periodic change of pressure distribution on the propeller blades. In this case, pressure in any point is changed periodically with rotation frequency but non harmonically. To measure pressure distribution on the rotating propeller at some angle of attack with reasonable quality, PSP has to transfer a few harmonics (about ten) of non harmonic pressure. Theoretical estimation of Amplitude-Frequency and Phase-Frequency Characteristics (AFC and PFC) for polymer-based PSP, well correlated with experimental results, show that AFC = 0.99 with PFC=-5^0 occurs at frequency $w=1.2/p^2t$, while at frequency 10ω, AFC = 0.68 and PFC=-35^0.[12] Value $\tau=4h^2/\pi^2D$ (h - PSP thickness, D - diffusion coefficient of PSP polymer) is a characteristic time of polyexponential relaxation of PSP signal on the pressure change. Ninety nine percent relaxation takes place in approximately 3τ, that is considered as Response Time of PSP. Thus for the pressure measurement on rotating propellers at nonzero angle of attack, PSP with response time less than 0.5 msec is needed. Creation of such PSP is a specific problem and is enough problematic for the polymer-based PSP. Fast response PSP may be created on the base of absorption layers, but possibility of application of such PSP in the wind tunnels must be carefully investigated, since its properties may be very sensitive to

humidity, fog, smoke, oil, solvents vapors etc. due to high surface activity of absorption layer.[16]

Experimental equipment

OPMS for T112 wind tunnel

The T112 wind tunnel has a rectangular 0.6m × 0.6m test section with a hole perforation on its sell and bottom and unperforated side walls. There are two different models. The first one is a wing with winglet, the second is the wing alone. The trapezoidal planform of the wing has a sweep at the quarter-chord of 30^0, an aspect ratio of 3.81, a taper ratio of 0.75, and a span of 0.4m. The winglet has also a tapered planform with a leading edge sweep of 30^0, an aspect ratio of 2.5, a taper ratio of 0.33, and a span of 0.2m. The wing and winglet are untwisted and have the same airfoil with thickness ratio of 9% and a roof-top type pressure distribution. Fig. 1 shows the relative position of the wing and the winglet. The model installation with the turning support placed on the test section side wall is shown in Fig. 2.

To determine a pressure distribution the inboard surface of the winglet and the part of the upper wing surface near its juncture were coated with the PSP LIPS18L1.[10] Light excitation of the paint active layer performed using impulse N_2 - laser and 4 optical fiber illuminators, which placed on the sell of the wind tunnel test section (see Fig.2). Two intensified CCD TV-cameras and a video recorder were taken to record the luminescence intensity field on the tested surfaces. The first TV-camera was placed on the same turning support as the model and the second was mounted on the test section sell.

OPMS for T106 wind tunnel.

Optical pressure measurement system for T106 wind tunnel was described in detail in our previous works.[9,11,13]

Left half wing of the model was painted by LPS L2. Pressure fields at angle of attack range from 10^0 to 20^0 presented existence of non stationary flow near leading edge. In this tests we used analog CCD camera coupled with video recorder. Acquisition rate was 25 frames per second what comply with estimations of the response time of PSP layer applied in this test ~ 0.1 sec.

System for PSP measurements on the propeller blade.

Prototype of a measurement system (Fig. 3) for application of PSP-technology to propellers was created and tested in T-104 wind tunnel.[24] Front surface of one blade of propeller was painted by Luminescent Pressure Sensor PSP L2 (produced by OPTROD Ltd., Russia), having luminescence decay time less than 0.5μsec and response time for the pressure change ~ 0.1 sec. To decrease additional weight, the polished blade was painted only by Active Layer of PSP without any Screen Layer. About 1g of PSP was applied on the blade of 500 cm^2 surface as a thin polymer layer (about 20μm thick).

During PSP application a set of markers and two spots of Luminescent Reference Film were placed on the model surface. Markers are contrasted points on PSP surface and are used for correction of model shape and position difference at reference and operating images during image processing. Luminescent Reference Film is insensitive to the pressure material and is used for correction of excitation light energy change at wind-on and wind-off conditions.

Pulsed light source was triggered by synchronization system at a certain position of painted blade. To get trigger pulse, beam of He-Ne laser, directed to the nose fairing of propeller, was reflected by small strip of reflective paper, attached at certain position on the nose fairing. Reflected light was detected by photomultiplier, whose signal after amplifier produced trigger pulse for initialization of pulsed light source. Total time delay of synchronization system was less than 1μsec. Digital CCD-camera with 512×512 pixels cooled array detected luminescent light. Optical glass filter was installed in front of camera lens to pass luminescent light and to cut off excitation light. This filter was carefully chosen to separate luminescence and excitation light effectively. Integrated images were digitized by 12-bit ADC and were stored and processed by PC486 computer.

Image processing was performed by a specially designed software. This software performs:

- Correction of distortion of operating image relative to reference image caused by model displacement and model deformation. This operation is performed by determination of geometrical correction function, allowing to get the best coincidence of the markers position on operating and reference images.
- Correction of excitation light intensity difference at operating and reference images. This operation is performed by factoring of operating image on the ratio of Luminescent Reference Film signal at the reference image to the one at the operating image.
- Calculation of pressure distribution on the model surface, using reference image, corrected operating image and calibration characteristic of PSP, determined in laboratory on the sample of the same PSP.

Discussion of the experimental results

Winglet operation

Winglet is a small, nearly vertical wing mounted at the tip of an airplane wing. (See Fig. 1.) The winglet is designed with carefully match between airfoil shape and local flow condition as the wing itself. The upper surface of this airfoil is the inboard surface. The winglet works in the circulation field of the wing tip, where the airflow tends to move outboard along the wing lower surface, around the tip, and inboard along the wing upper surface. This wing-tip vortex produces a cross flow at the winglet, and the winglet produces a large side force because the vortex intensity is not small for real airplane. Since the side force

vector is approximately perpendicular to the local flow, the side force has a forward component that reduces the airplane induced drag. To increase the winglet benefit the side force must be as large as possible; therefore, airfoil with high lift is used. The thrust produced by the winglet depends upon the strength of the circulation around the wing tip and is larger for those airplanes with higher wing loads near the tip.

The notion of the winglet operation allows to point how the typical wing-tip flow can be changed. The side force results from rarefaction on the inboard winglet side, therefore an additional rarefaction domain occurs on the upper wing surface. Its length along the wing is in the order of the winglet root chord. This is the main property of the flow near the wing-winglet juncture. It leads to the more intensity flow deceleration in the trailing edge region and as a consequence to the earlier flow separation than in the case of the wing alone. If a shock wave appears in the flow, it is shifted downstream by this rarefaction domain. The wing-tip vortex cross flow disappears in the region.

The winglet flow is primarily governed by the wing-tip vortex and the winglet position relative the wing, and it is not so complicated as the wing one. Because the induced cross flow velocity decreases monotonically from the root to the tip, the largest rarefaction is on the root part of the winglet if the last is untwisted. The wing-winglet interaction can not drastically change this condition.

The luminescence intensity field of the paint detected some periodical low frequency motions of the shock wave. Special procedure was developed to obtain the frequency of the shock wave periodical movement. For this object the digital spectral analysis is employed to 168 successive video frames, which are digitized and registered using image acquisition system.

The time sequence element is obtained by using two-dimensional windows in each frame:

- window with the information about the oscillated shock position located behind the shock,
- window with the information about a background intensity located before the wing,
- window of a reference plate which luminescence intensity is not pressure sensitive and reflects the optical channels transmission variation.

The data in the windows of each frame are averaged to improve a signal-to-noise ratio and three arrays: measured, reference, and background are performed. Then we subtract the background from the measured and reference values and divide the measured values by the reference ones. This provides the elimination of both background fluctuations and optical channels transmission variation. The number of the sequence elements taken as 168 agrees with the capabilities of the system frame buffer. The shock oscillation frequency is determined by the maximal value of the power spectral density. The direct method of the spectral density estimation, which is a discrete Fourier Transformation, does not ensure an acceptable accuracy because the number of the time sequence and the signal-to-noise ratio are small. In this condition the best result can be obtained by the parametric description of the input data by ARMA (AutoRegression and Moving Average) method.[6]

Tests have been held for free-stream Mach number of 0.6, 0.75, 0.8, 0.85 and 0.9 and angle of attack a ranged from 0^0 to 12^0 . Herein we present the data only for Mach number of 0.75 and 0.85. The first group of the data is typical for transonic flows with small supersonic domains or without them, and the second -- for flows with moderate supersonic domains and shock waves. All the results are displayed as constant value lines of the pressure coefficient on the tip part of the wing upper surface and on the winglet inboard surface.

Figure 3 shows the flows around the wing alone at Mach number of 0.75 and the angle of attack of 4^0, 6^0, and 10^0. At $\alpha=4^0$ we see a typical pressure distribution for the case of a moderate loaded wing tip and subsonic velocity on its leading edge (M=0.95). At $\alpha=6^0$ the load is increased, and the leading edge velocity becomes supersonic (M=1.3). The pressure rises downstream but does not restore at the trailing edge. That does not mean a flow separation and is due to the wing-tip vortex induced velocity. According to the numerical and experimental study the velocity is the highest at the trailing edge and decreases rapidly when going out from the wing tip.[7] This low pressure region is well seen in the figure. At $\alpha=10^0$ the region is extended. At this angle of attack the leading edge velocity (M=1.45) is large enough to cause a shock induced boundary layer separation. We see from the pressure distribution that if the separation occurs, it is followed by reattachment and the flow over the wing end is unseparable in the whole.

Figure 4 shows the flows around the wing with the winglet at the same Mach number and angles of attack. At $\alpha = 4^0$ we see the main difference from the flow over the wing alone in the figure 4 is the additional rarefaction which occurs due to the winglet flow.

The size of the rarefaction region and the pressure level in it are well seen in the figure. At $\alpha=6^0$ the level of rarefaction becomes higher, but the size does not change noticeably. There is also a difference between the flows in the rear part of the wing. It appears because the winglet cuts the wing-tip vortex and the velocities field is changed in this domain. Nevertheless the pressure distribution, which is partly controlled by the flow on the wing down surface, is nearly varied there at $\alpha=6^0$. At $\alpha=10^0$ this winglet action leads to the more noticeable change in the pressure distribution in the whole wing-winglet juncture region, but it is very difficult to explain the behavior of the data in figure 5 by the action only. Probably, the flow is separated at this condition, and our insight into the problem based on a linear theory become invalid.

The pressure distributions on the winglet inboard surface are shown in figure 5 at the same Mach number and angles of attack. Qualitatively they look as in the flow

around the tapered wing with the special twist which simulates the variation of the cross flow velocity induced by the wing-tip vortex. At $\alpha=4^0$ and $\alpha=6^0$ the data in figure 6 agree in the whole with our look on the flow in which the wing vortex system is responsible for the interaction. The absence of the agreement at $\alpha = 10^0$ also indicates that the viscous influence is very important at this condition.

When looking through the recorded data of the tests as a movie we have seen a periodical shock wave movement near 1/3 chord of the wing upper surface in the wing-winglet flow at free-stream Mach number of 0.8 and 6^0 angle of attack.. The amplitude of the motion was about 5%. The numerical treatment of the data by the procedure described above allows to estimate the frequency of the shock wave movement as 1.02 s. This result shows that unsteady motions can arise in the wing-winglet flow, and LIPS method is applicable to detect them.

Results for training aircraft model.

In order to obtain low frequency pressure field variations 40 successive video frames were digitized and stored in the video buffer. Reference images were acquired after wind tunnel run. In these tests model was suspended on X-shaped support bands so it was necessary to compensate only small side board displacements of the model. Image alignment procedure as well pressure field calculation were performed in batch mode for each forty frames series.

Time evolution of the pressure field was more apparent at Mach number 0.7. C_p fields presented on Fig. 6 and Fig. 7 have been chosen to show maximum detectable variations in C_p field topologies. Pike decompression zone near leading edge at AOA $\alpha=10^0$ are usually divided in two parts (sometimes three) with boundary point attached to the leading edge and migrating along it. C_p distributions along wing span at 5% of local wing chord are presented on Fig. 8 and 9 demonstrate the magnitude of spatial and amplitude fluctuations. C_p fields at AOA $\alpha=20^\circ$ (Fig. 9) show separated flow having more conservative topology with fluctuation in amplitude mainly.

Results for propeller blades.

Described measurement system, with nitrogen pulsed laser as excitation light source, was used to measure pressure distribution on the front surface of rotating blades of two models of propellers in subsonic airflow of T-104. T-104 is an open-jet subsonic wind tunnel of 7 meters nozzle diameter allowing to get flow speed in the range of 0÷120 m/sec.

The first model was twin-blade propeller model of 0.65m diameter having sweptback blades from the first rotor of coaxial propeller CB-27M. The model was investigated in whole flow speed range of T-104 wind tunnel at rotation frequency 7000r pm at different installation angles of blades $\beta=15^0$, 22.5^0, 30^0, 40^0 (β - blade installation angle at relative radius r/R=0.75). This rotation frequency of propeller model corresponds to the full scale blade speed. Fig. 10 presents pressure distributions on the blade installed at the angle $\beta=40^0$ at different flow speeds V=20, 40, 60, 90 m/sec, and Fig. 11 presents pressure distributions on the blade installed at different angles β $=15^0$, 22.5^0, 30^0 at the absence of the flow. These figures show the change of flow structure about blade surface depending on installation angle and flow speed.

The second model was twin-blade propeller model of 0.85m diameter having the blades from the propeller AB-36C. Real propeller has 6 blades and is designed for low range aircraft for flight speed at Mach number 0.3. The model was investigated in whole flow speed range at rotation frequency 5300 rpm at different installation angles of blades β=-10^0, 5^0, 10^0, 15^0, 20^0, 25^0, 35^0, 45^0. This rotation frequency of propeller model corresponds to the full scale blade speed. Fig. 12 presents pressure distributions on the blade installed at the angle $\beta=45^0$ at different flow speeds V=30, 60, 90, 113m/sec, and Fig. 13 presents pressure distributions on the blade installed at different angles β=-10^0, 15^0, 35^0, 45^0 at the absence of the flow. Similarly to the previous figures, these figures show the change of flow structure about blade surface depending on installation angle and flow speed. Pressure patterns on the blade show that at some conditions few stalls may appear on the upper surface of the blade. Intensity of the stalls decreases with the increase of flow speed and at some speed the flow about blade surface becomes nonstalled.

Finally, an attempt to measure pressure distribution on rotating blade at nonzero angle of attack of rotation axis was made. For this purpose, the second blade of AB-36C propeller was covered by Luminescent Pressure Sensor LPS F1 (OPTROD Ltd., Russia), having shorter response time than LPS L2 - 5 msec, while this response time is not enough short for precise measurement of periodic component of pressure on rotating blades at frequency 5300 rpm. Measurements were made at flow speeds in the range of 0÷60 m/sec on the blade installed at the angle β $=20^0$ at the angles of attack α=-4^0, 0^0, 4^0, 10^0 Pressure distributions were measured at blade position corresponding to the largest periodical pressure component. According to the estimations, periodic pressure component does not exceed 1.5÷2% of mean pressure, i.e. it is of the same value as an error of pressure measurement in these tests. So, the conducted experiments do not allow to estimate the feasibility to use LPS F1 for pressure measurements on rotating blades at nonzero angles of attack.

Conclusions

(1). Pressure Sensitive Paint permits to investigate unsteady separated flow on the aircraft models.

(2). The presented results prove that PSP technology is extremely attractive method of pressure measurements on rotating blades, fast enougth, cheap and universal.

References.

1. Whitcomb R.T, "A design Approach and Selected Wind Tunnel Results at High Subsonic Speeds for Wing-Tip Mounted Winglets", NASA TN D-8260, July, 1976.
2. Flechner S.G., Jacobs P.F. "Experimental Results of Winglets on First, Second, and Third Generation Jet Transports", NASA TM 72674, May, 1978.
3. Montoya L.C. Flechner S.G. Jacobs P.F. "Effect of an Alternative Winglet on the Pressure and Spanwise Load Distributions of a First-Generation Jet Transport Wing", NASA TM 78786, December, 1978.
4. Ishimitsu K.K. "Aerodynamic Design & Analysis of Winglets" AIAA Aircraft Systems and Technology Meeting, Dallas, Texas, September, 27-29, 1976.
5. Чичеров Н.А. Некоторые результаты параметрических исследований крыльев с концевыми шайбами. Труды ЦАГИ, вып. 2504. М. 1991.
6. Marple-Jr. S.L. "Digital Spectral Analysis", Prentice-Hall Inc., 1987.
7. Barinov D.A. et al "Flow Field Investigations in the vicinity of the tip of a sweep wing." Uchenye Zapiski TsAGI, v.9 N2, 1980. (in Russian)
8. Majkapar G.I., Keldysh V.V., "Results of investigation of pressure-taped propellers", Set of reports on the theory of propellers, TsAGI 1958, pp. 240-258, (in Russian).
9. Bykov A.P., Orlov A.A., Mosharov V.E., Pesetsky V.A., Radchenko V.N., Sorokin A.V., Fonov S.D., Alaty L., Colucci V. "Application of Luminescence Quenching for Pressure Field Measurements on the Model Surface in a Wind Tunnel", conference "Wind Tunnels and Wind Tunnel Testing Techniques", South Hempton, September 1992.
10. Troyanovsky I., Sadovskii N., Kuzmin M., Mosharov V., Orlov A., Radchenko V., Fonov S. "Set of Luminescence Pressure Sensors-LIPS for Aerospace Research.", 1st European conference on optical chemical sensors and biosensors, Graz, Austria 12-15 April 1992. Sensors and Actuators B, 11 (1993) 201-206.
11. Bykov A., Mosharov V., Orlov A., Pesetsky V.A., Radchenko V., Matyash S., Fonov S., Kuzmin M., Sadovskii N., "Optical surface pressure measurements: accuracy and application field evaluation" 73rd AGARD Fluid Dynamics Panel Meeting and Symposium on Wall Interference, Support Interference and Flow Field Measurements, Brussels, Belgium 4-7 October 1993.
12. Mosharov V., Orlov A., Radchenko V., Kuzmin M., Sadovskii N., "Luminescent Pressure Sensors for Aerospace Research: Diffusion-Controlled Characteristics", 2nd European conference on optical chemical sensors and biosensors, Firenze, Italy, 19-21 April 1994.
13. Andreev A.O., Bykov A.P., Ipatov M.W., Kabin S.V., Nushtaev P.D., Orlov A.A., Mosharov V.E., Radchenko V.N., Pesetsky V.A., Fonov S.D., "Pressure fields investigation by LPS technology on the aerospacecraft model", J.Phys.III France 4 (1994) 2317-2337.
14. Kavandi J., Callis J., Gouterman M., Khalil G., Wright D., Green E., Burns D., McLachlan B. "Luminescent Barometry in Wind Tunnels.", Rev. Sci. Instruments, 61(11), pp. 3340-3347, November 1990.
15. McLachlan B.G., Kavandi J.L., Callis J.B., Gouterman M., Green E., Khalil G, "Surface pressure field mapping using luminescent coatings", Experiments in Fluids 14, 33-41(1993).
16. Baron A.E., Danielson J.D.S., Gouterman M., Wan J.R., McLachlan B., "Submillisecond response times of oxygen-quenched luminescent coatings", Rev. Sci. Instrum. 64 (12), Dec. 1993.
17. Crites R.C., Benne M.E., Morris M.J., Donovan J.F. "Optical Surface Pressure Measurements: Initial Experience in the MCAIR PSTWT", conference "Wind Tunnels and Wind Tunnel Testing Techniques", South Hempton, September 1992.
18. Morris M.J., Donovan J.F. "Application of Pressure- and Temperature - Sensitive Paints to High-Speed Flows", 25th AIAA Fluid Dynamics Conference, June 20-23, 1994/ Colorado Springs, CO, AIAA 94-2231.
19. Jagharhi A.J., Mitchell M., Burkett C., Sealey S. "Wind Tunnel Application of Pressure Sensitive Paint at NASA Langly Research Center (8-foot TPT & 7'x10' HST)", NASA LaRC IRD ATMB, June 15, 1993.
20. Sellers M.E., Brill J.A., "Demonstration Test of Pressure Sensitive Paint in the AEDC 16-ft Transonic Wind Tunnel Using the TST Model", 18th AIAA Aerospace Ground Testing Conference, June 20-23, 1994/ Colorado Springs, CO, AIAA 94-2231.
21. Engler R. H., Hartmann K., Schulze B. "Aerodynamic Assessment of an Optical Pressure Measurement System (OPMS) by Comparison with Conventional Pressure Measurements in High Speed Wind Tunnel", 14th ICIASF Congress, October 27-31, 1991, Rockville, MD.
22. Burns S.P., Sullivan J.P., "The Use of Pressure Sensitive Paints on Rotating Machinery", 16th ICIASF Congress, July 18-21, 1995, Dayton, Ohio.
23. Lifshitz Yu., Fonov S., Morozov A., Orlov A. Radchenko V., Pesetski V. "A Study of Transonic Winglet-Wing Flow with Light Intensity Pressure Sensors", TsAGI's preprint N 78, 1993
24. Bykov A, Fonov S, Kishalov A, Mosharov V, Orlov A, Ostroukhov S., Radchenko V., "Application of Luminescent Pressure Sensor Technology to Propellers". TsAGI's preprint N 101, 1995.

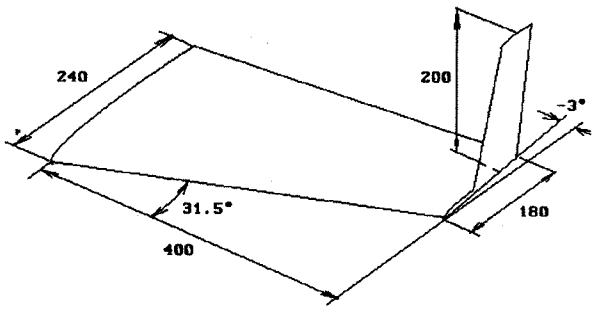

Fig. 1 The wing-winglet geometry

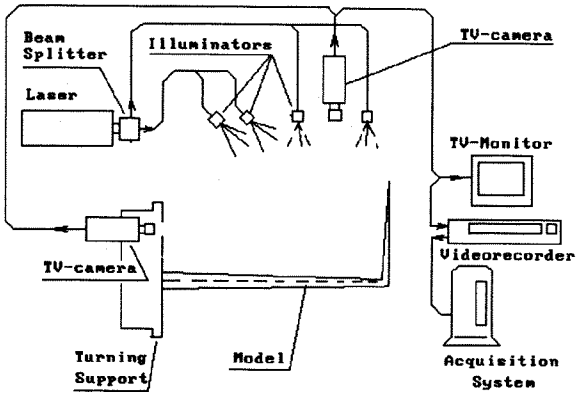

Fig. 2 The measurement system setup.

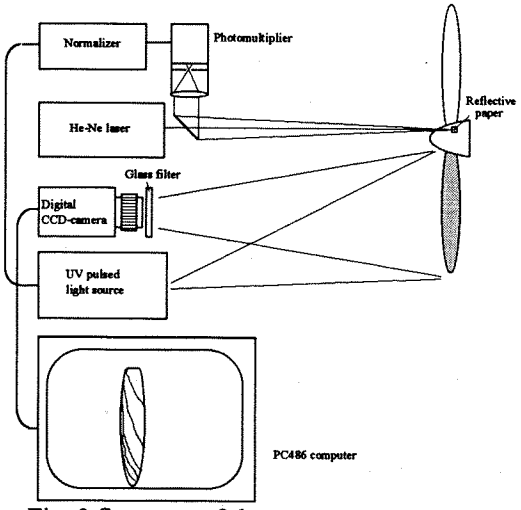

Fig. 3 Structure of the measurement system for application of PSP-technology on propellers.

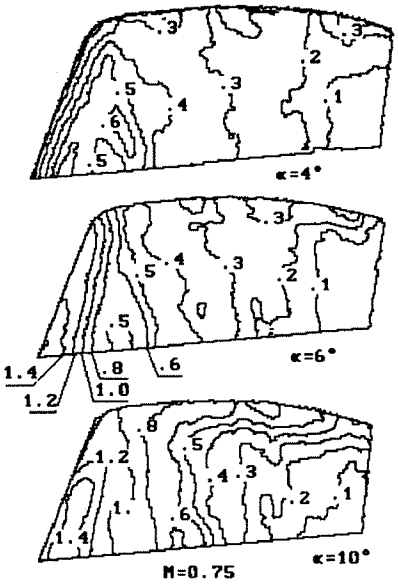

Fig. 3 Level lines of the pressure coefficient ($-C_p$) on the wing upper surface
in the wing alone flow at M_{oo}=0.75.

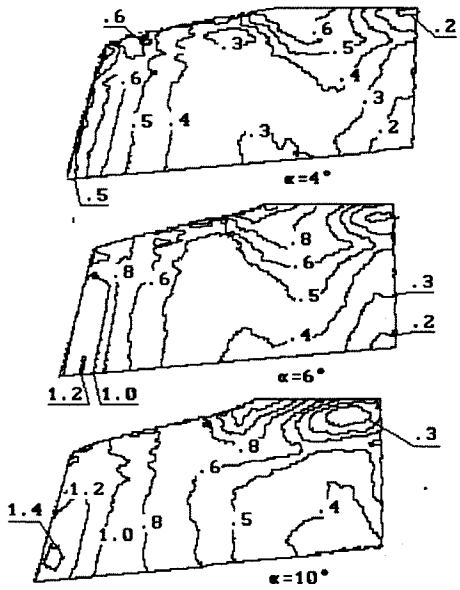

Fig. 4 Pressure coefficient ($-C_p$) on the wing upper surface in the wing -winglet flow at M_{oo}=0.75.

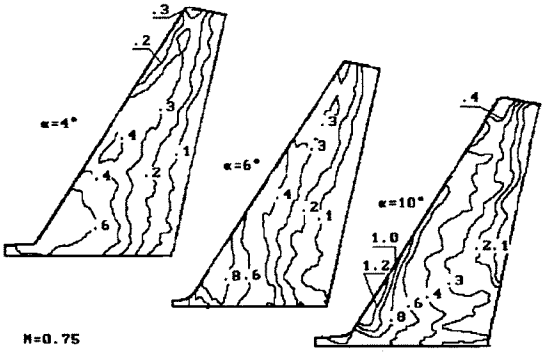

Fig. 5. Pressure coefficient ($-C_p$) on the winglet upper surface in the wing -winglet flow at M_{oo}=0.75.

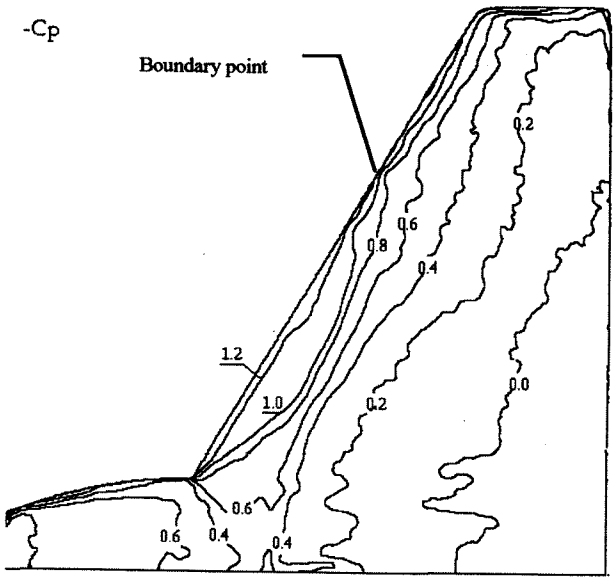

a.

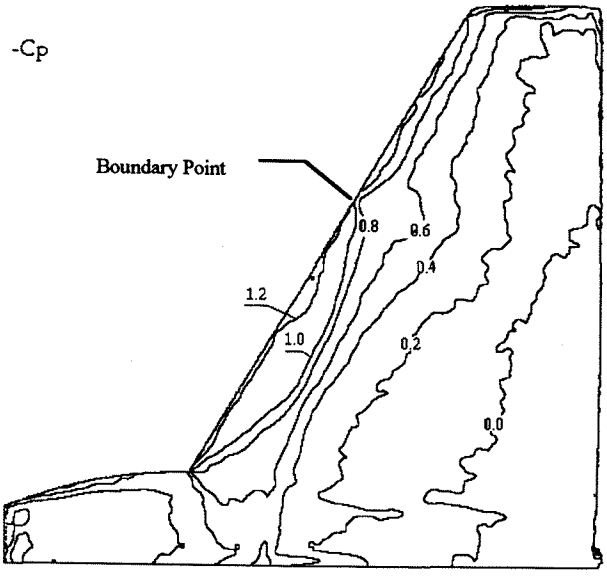

b.

Fig. 6 C_p fields at M=0.7 α=10°

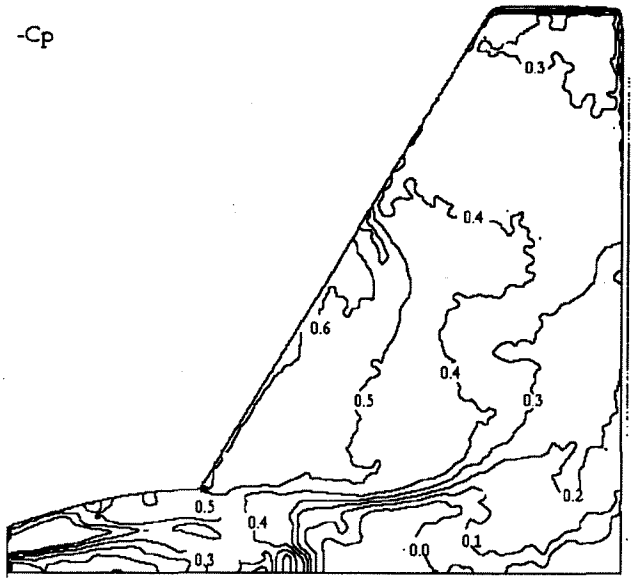

a.

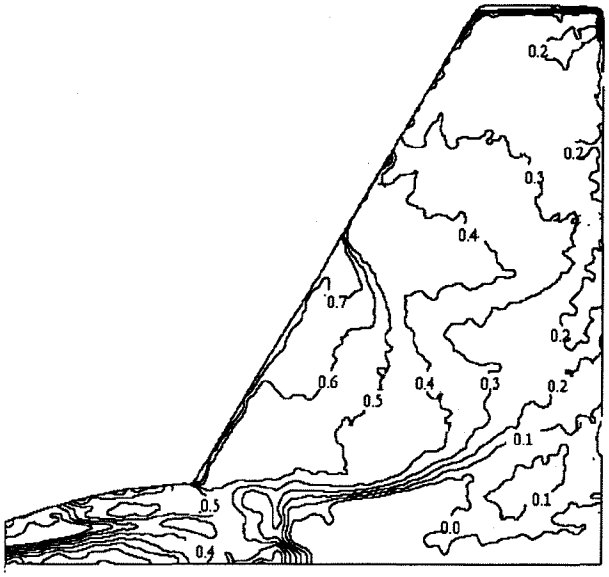

b.

Fig. 7 C_p fields at M=0.7 α=20°

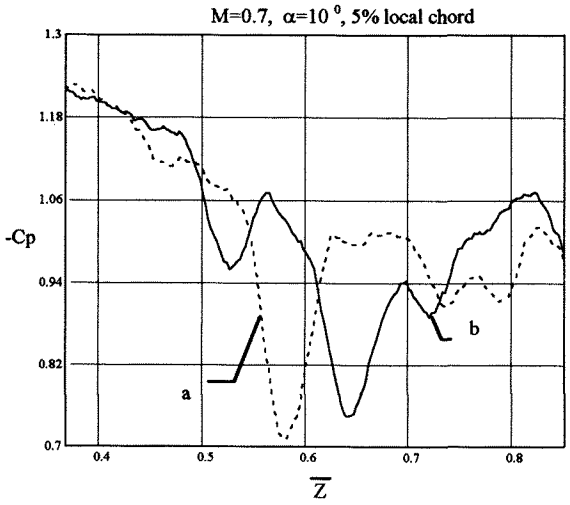

Fig. 8 C_p distributions along 5% chord line.

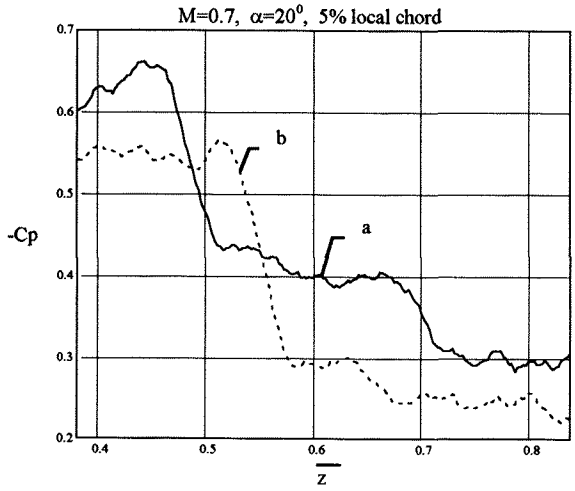

Fig. 9 C_p distributions along 5% chord line.

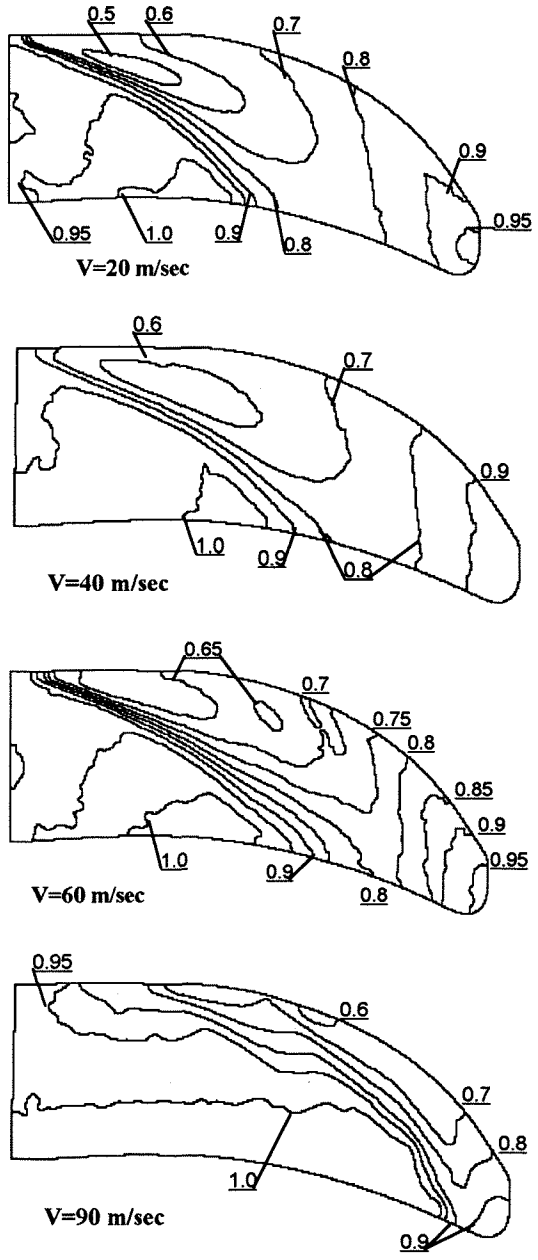

Fig. 10. Pressure distributions (in *bars*) on a blade of CB-27M propeller at installation angle $\beta=40^{o}$ and rotation frequency $n=7000$ *rpm* at different flow speeds.

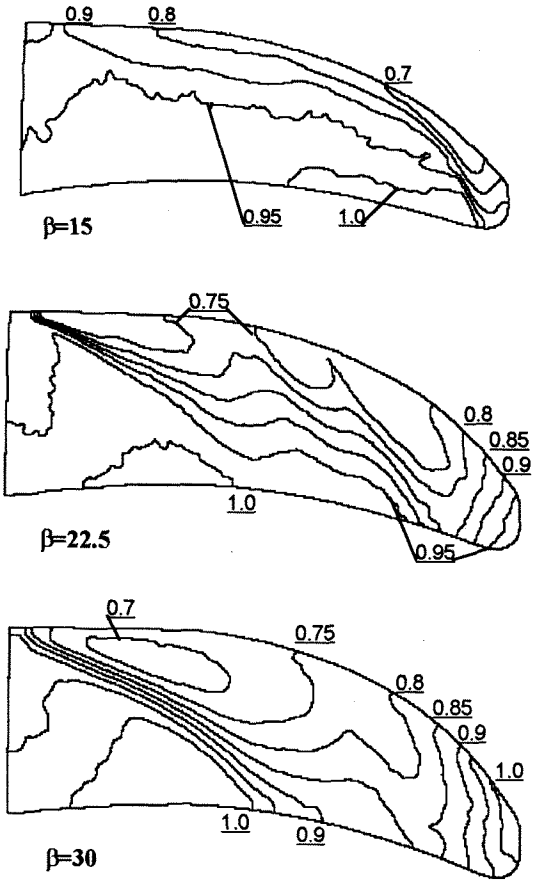

Fig. 11. Pressure distributions (in *bars*) on a blade of CB-27M propeller at zero flow speed and rotation frequency *n=7000 rpm* at different installation angles.

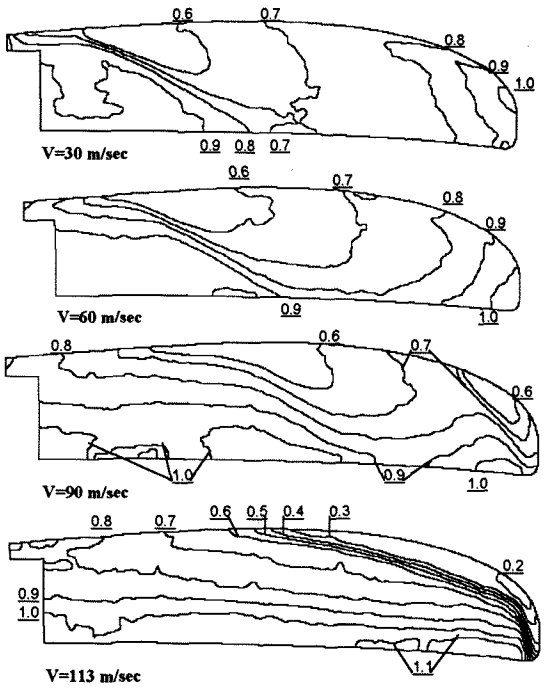

Fig. 12. Pressure distributions (in *bars*) on a blade of AB-36C propeller at installation angle $\beta=45^{o}$ and rotation frequency *n=5300 rpm* at different flow speeds.

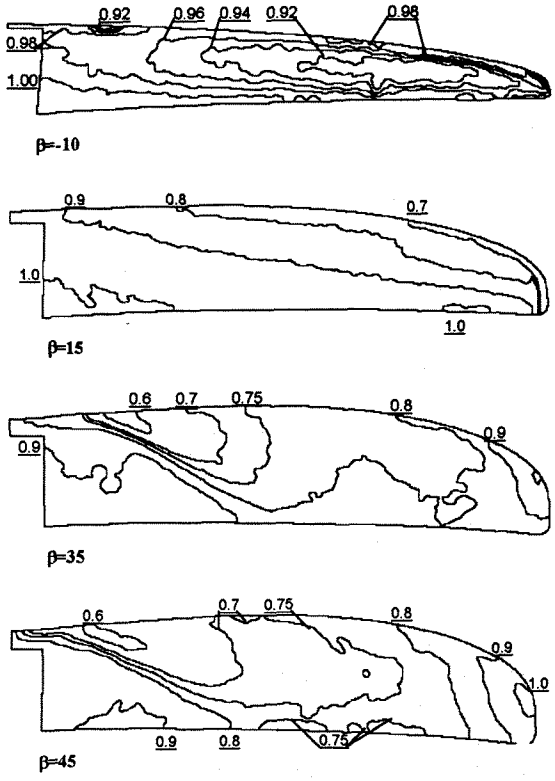

Fig. 13. Pressure distributions (in *bars*) on a blade of AB-36C propeller at zero flow speed and rotation frequency *n=5300 rpm* at different installation angles.